ELSEVIER

Contents lists available at SciVerse ScienceDirect

Journal of Alloys and Compounds

journal homepage: www.elsevier.com/locate/jalcom



Spin dynamics evidenced by EPR in $Sn_{1-x}Mn_xO_2$ nanoparticles annealed at different temperatures

A. Popa a, D. Toloman a, O. Raita a,*, M. Stan B.S. Vasile b, C. Leostean L.M. Giurgiu a

- ^a National Institute for Research and Development of Isotopic and Molecular Technologies, Donath 65-103, 400293 Cluj-Napoca, Romania
- ^b University "Politennica", Faculty of Applied Chemistry and Material Science, Department of Science and Engineering of Oxide Materials and Nanomaterials, 1-7 Gh. Polizu, 011061 Bucharest, Romania

ARTICLE INFO

Article history: Received 31 July 2012 Received in revised form 28 September 2012 Accepted 3 October 2012 Available online 12 October 2012

Keywords: Nanostructured materials Liquid-solid reactions Electron paramagnetic resonance Transmission electron microscopy

ABSTRACT

This article reports the effects of the annealing temperature on the structural, morphological and spin dynamic properties of SnO_2 samples doped with 0.005 Mn. The samples were annealed at 400, 600, 700 and 800 °C and analyzed by XRD, TEM, XPS and EPR spectroscopy. The XRD spectra show that the average crystallite size increases with the increase of the annealing temperature. The particles size and morphology were characterized by TEM microscopy. The valence bands of Mn were investigated by measuring the XPS spectra of Mn 2p core-level doublet. Regardless of the annealing temperature, the observed EPR spectra are due to (i) Mn^{2+} ions either interstitially situated on the particle surfaces or isolated ones located substitutionally at Sn sites and (ii) Mn^{4+} ions which substitute for Sn^{4+} in SnO_2 lattice. The effects of the annealing temperature on the relative fractions of Mn^{2+} and Mn^{4+} ions are presented and discussed. In $Sn_{1-x}Mn_xO_2$ (x=0.005) sample annealed at 400 °C, a FMR line was identified and attributed to a ferromagnetic phase.

© 2012 Elsevier B.V. All rights reserved.

1. Introduction

In the research area of materials with high ferromagnetic Curie temperatures and with controllable spin properties, DMSs oxides such as TiO₂, ZnO, SnO₂, doped with transition-metal ions (Mn, Fe, Co, Ni, Cr, etc.) have attracted considerable attention.

Due to its wide band gap (3.60 eV), transition-metal-doped SnO_2 is expected to play an important role in multidisciplinary areas of materials science and future spintronic devices [1]. Doping SnO_2 with transition-metal elements is one of the most popularly used approaches to tune the performance of SnO_2 material.

It was demonstrated that the preparation method and the synthesis conditions are very important in stabilizing the ferromagnetic behavior required in applications [2,3]. In this context, it has been reported that the annealing of the TM-doped oxide influences the magnetic properties of the DMS materials [4–9]. However, a complete understanding of the influence of annealing on the properties of DMS system has not yet been accomplished.

The aim of the present work is to understand the role of annealing temperature on the incorporation of Mn into the lattice of SnO₂. The study is concentrated on the Electron Paramagnetic Resonance (EPR) analysis of the $\mathrm{Sn}_{1-x}\mathrm{Mn}_x\mathrm{O}_2$ powders. This technique is usually employed to study the change of structure, lattice defects, and distortions.

By means of EPR, one can determine the valence state of Mn ions in $Zn_{1-x}Mn_xO$ systems, fact which is required for explaining the origin of ferromagnetic order.

2. Experimental

A series of SnO_2 powders doped with Mn^{2+} ions having the formula $Sn_{1-x}Mn_xO_2$ with (x = 0.005) were synthesized as follows.

The $Sn_{1-x}Mn_xO_2$ samples were synthesized using tin(II) oxalate $(SnC_2O_4$ for synthesis, Merck) and manganese(II) nitrate tetrahydrate $(Mn(NO_3)_2.4H_2O$ 98.5%, GR for analysis, Merck). The appropriate stoichiometric quantities were dissolved in distilled water and the mixture obtained was stirred about 1 h for homogenization. Afterwards, the reaction mixture was decomposed at 250 °C in air until dry. The temperature was raised gradually over 2–3 days. After heat treatment the mass precursor was ground to give fine powder.

After preparation, fractions of the obtained powders were calcined at different temperatures (400, 600, 700 and 800 °C) for 2 h by oxidation in air and will be subjected to subsequent physical measurements.

X-ray diffraction (XRD) patterns were recorded using a high-resolution Bruker D8 Advance diffractometer with Cu X-ray tube and incident beam Ge (111) monochromator (λ = 1.54056 Å).

The bright field and high resolution images coupled with SAED (selected area electron diffraction) were obtained using a Tecnai G^2 F30 S-TWIN transmission electron microscope (FEI, the Netherlands), equipped with a STEM/HAADF detector. The microscope operates at an acceleration voltage of 300 kV (Shottky field emitter) with a TEM point resolution of 2 Å nm and a TEM line resolution of 1 Å.

X-ray photoelectron spectroscopy (XPS) was carried out on a VG Scientific ESCA-3 Mk II spectrometer having as X-ray source the Al Ka radiation (1486.6 eV, non-monochromatic) of an anode operating at 14 kV and 20 mA.

EPR measurements of the powder samples were performed with a Bruker ELEX-SYS 500 spectrometer operating at X-band (9.52 GHz) and Q-band (34.08 GHz) frequencies. The mesurements were done using the following experimental

^{*} Corresponding author. Tel.: +40 264 584 037; fax: +40 264 420 042. E-mail address: oana.raita@itim-cj.ro (O. Raita).

parameters were: microwave power, 2 mW; modulation frequency of 100 kHz and a magnetic field modulation amplitude of 10 G. The spectra were acquired at low temperatures and room temperature. The processing was performed by Bruker Xepr software. The EPR spectra were recorded using equal quantities of samples.

3. Results and discussion

Fig. 1 shows XRD patters for the $\mathrm{Sn}_{1-x}\mathrm{Mn}_x\mathrm{O}_2$ (x=0.005) sample annealed at $T_{\mathrm{an}}=400$, 600, 700 and 800 °C. Obviously, the XRD peaks of the Mn doped SnO_2 sample are identical to those of pure SnO_2 rutile-type tetragonal phase.

As can be seen in Table 1, the average crystallite size, calculated along (101) direction, increases with the increase of the annealing temperature for analyzed samples. This behavior was also observed by other researchers as well [10–12].

The particles size and morphology were characterized by TEM microscopy. As an example, the images of $\mathrm{Sn}_{1-x}\mathrm{Mn}_x\mathrm{O}_2$ (x = 0.005) annealed at different temperatures are shown in Fig. 2. We have observed an agglomeration of the individual particles and the smallest nanoparticle diameter was obtained for the sample annealed at 400 °C. The mean size of individual particles is 8, 23, 25 and 28 nm for the samples annealed at 400, 600, 700 and 800 °C, respectively.

The nanoparticle's diameters are comparable with the crystallite dimensions calculated from RDX. A representative high resolution TEM (HRTEM) image is given in Fig. 3.

Lattice fringes are clearly visible from this image, revealing its single crystalline nature. The interplanar spacing are approximately 0.237 nm for the (020) planes of tetragonal rutile SnO_2 [13].

The valence bands of Mn were investigated by measuring the XPS spectra of Mn 2p and Sn 3d core-levels. In both cases of p and d core-levels lines, the restrictions used for the fit of XPS spectra refer to the usual relation between areas of doublet components. By using CASA software the integral intensities were calibrated using real sensitivity, transmission and electronic mean free path factors.

For exemplification in Fig. 4 is presented the deconvoluted Mn 2p spectra corresponding to the sample annealed at $800\,^{\circ}$ C. Mn 2p core-level binding energies spectra show $\mathrm{Mn^{2^+}}$ doublet lines 3/2 and 1/2 at about 640.65 and $651.76\,\mathrm{eV}$ respectively (peaks labeled A on the figure) while the positions at 642.0 and $653.1\,\mathrm{eV}$ are corresponding to $\mathrm{Mn^{4^+}}$ (peaks labeled B on the figure). As expected, additional satellite peaks were also evidenced [14–16]. The intense line between the doublets has no physical significance being the

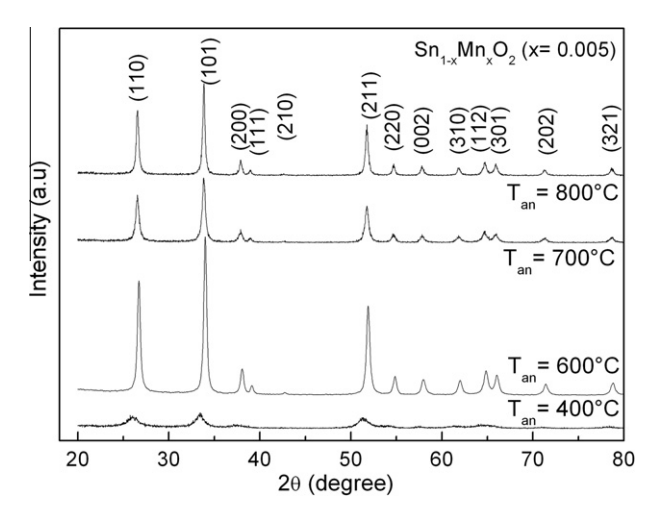


Fig. 1. XRD patterns of $Sn_{1-x}Mn_xO_2$ (x = 0.005) as function of the annealing temperature.

Table 1 The crystallite dimension, d, as function of annealing temperature, $T_{\rm ann}$, calculated along the (101) direction.

<i>T</i> _{an} (°C) <i>d</i> (Å)	400	600	700	800
d (Å)	73	220	235	261

cumulative contribution of choosing a linear background and asymmetries of spectral lines. The veracity of Mn 2p core-level lines deconvolution was tested by calculating the doping degree relatively to Sn 3d. The determined values are consistent with those used in the preparation sample process ($\sim 0.5\%$).

XPS spectra enabled us to calculate the concentration of $\rm Mn^{4^+}$ and $\rm Mn^{2^+}$ ions relative to the total concentration of Mn from the sample. The results are presented in Table 2. We have observed that the relative concentration of $\rm Mn^{2^+}$ increases by increasing the annealing temperature, going through a maximum at 600 °C and then decreases abruptly.

For a deeper understanding of the influence of annealing temperature on $\mathrm{Sn}_{1-x}\mathrm{Mn}_x\mathrm{O}_2$ (x=0.005) EPR measurements were performed. In Fig. 5 we present a comparison of the EPR spectra corresponding to the samples annealed at different temperatures. The EPR spectra were measured at 300 K.

Three paramagnetic oxidation states for incorporated manganese ions in SnO_2 can exist: Mn^{2+} ($3d^5$, S = 5/2), Mn^{3+} ($3d^4$, S = 2) and Mn^{4+} ($3d^3$, S = 3/2). One expects a characteristic hyperfine structure of six lines because the only natural isotope ⁵⁵Mn (100% abundant) has a nuclear spin, I = 5/2.

An inspection of these spectra shows the presence of three important centers. The first center corresponds to the multiple-line spectrum located at the lower-field side in Fig. 5 (inset). This center is due to the $\mathrm{Mn^{4+}}$ ions which substitute for $\mathrm{Sn^{4+}}$ ions in $\mathrm{SnO_2}$. The second center consists of a symmetric broad line with g = 2.000 attributed to the interstitial $\mathrm{Mn^{2+}}$ ions situated on the particle surfaces. The third center with the six line hyperfine structure could arise from the paramagnetic moments of the isolated $\mathrm{Mn^{2+}}$ ions located substitutionally at Sn sites in $\mathrm{SnO_2}$ lattice. A more detailed discussion concerning the assignment of Mn centers observed by EPR in $\mathrm{Sn_{1-x}Mn_xO_2}$ samples can be found elsewhere [17]. In X-band spectra presented in Fig. 5, the hyperfine structure is not well resolved and it is superimposed on the second center.

For obtaining a better resolution of the third center, a Q-band EPR spectrum at room temperature was recorded. In Fig. 6 is presented the EPR spectrum of this center in $\mathrm{Sn}_{1-x}\mathrm{Mn}_x\mathrm{O}_2$ (x = 0.005) sample annealed at 400 °C.

A more detailed analysis of the X-band and Q-band EPR spectra of $Sn_{1-x}Mn_xO_2$ (x = 0.005) sample annealed at 400 °C, reveals that this sample presents an additional quite broad resonance line (marked by arrows in Figs. 5 and 6). This signal was also observed by other researchers in ZnO diluted magnetic semiconductor [18] and will be discussed later.

In order to describe the evolution of the Mn²⁺ and Mn⁴⁺ ion concentrations with annealing temperature, we introduce the relative fractions of the corresponding ions which are given by [17]:

$$f_r^{\mathrm{Mn}^{2+}} = \frac{c_{\mathrm{S}}^{\mathrm{Mn}^{2+}}}{c_{\mathrm{S}}^{\mathrm{Mn}^{2+}} + c_{\mathrm{S}}^{\mathrm{Mn}^{4+}}}$$

$$f_r^{\text{Mn}^{4+}} = \frac{c_S^{\text{Mn}^{4+}}}{c_S^{\text{Mn}^{2+}} + c_S^{\text{Mn}^{4+}}}$$

Here, $f_r^{\mathrm{Mn}^{2+}}$ represents the relative fraction of all Mn^{2+} ions, either interstially situated on the particle surfaces or substitutionally isolated ones, with respect to that of the total EPR spectrum and $c_S^{\mathrm{Sn}^{2+}}$ is the corresponding spin concentration. Similarly for Mn^{4+} ions, $f_r^{\mathrm{Mn}^{4+}}$ and $c_S^{\mathrm{Mn}^{4+}}$ are the relative fraction and spin concentration, respectively.

Download English Version:

https://daneshyari.com/en/article/1614989

Download Persian Version:

https://daneshyari.com/article/1614989

<u>Daneshyari.com</u>